DISCLAIMER

UCRL-1133
Unclassified-Physics Distribution
Copy 2

UNIVERSITY OF CALIFORNIA

Radiation Laboratory

Contract No. W-7405-eng-48

SUMMARY OF THE RESEARCH PROGRESS MEETING OF FEBRUARY 8, 1951

Bonnie E. Cushman

March 8, 1951

"Some of the results reported in this document may be of a preliminary or incomplete nature. It is the request of the Radiation Laboratory that the document not be circulated off the project nor the results quoted without permission."

Berkeley, California

SUMMARY OF THE RESEARCH PROGRESS MEETING, FEBRUARY 8, 1951

Bonnie E. Cushman

March 8, 1951

Measurement of decay electron spectrum from μ^+ mesons by means of the spiral orbit spectrometer focusing - R. Sagane.

Previous studies of the decay electron spectrum have not been accurate enough to determine which coupling theory holds. Tiomno, Wheeler and Rau have reviewed the work done on this problem up to 1949 (see Reviews of Modern Physics 21, 144-52 (1949)), assuming that the decay is a three particle process: $\mu \rightarrow \mu_0 + \nu^- + e$, or in a special case: $\mu \rightarrow 2\nu^- + e$. They conclude that some new experimental technique is needed to discriminate between the theories; it is hoped that the development of the spiral spectrometer will satisfy this need.

The idea for the instrument was suggested in 1941 by Dr. Sagane's student, Miyamoto. The operating principle involves an asymmetric heterogeneous magnetic field, provided in the present experimental arrangement by putting together a Mozely magnet and a horizontal cloud chamber magnet. One can then measure the energy spectrum of the electrons by varying the magnetic field. Electrons with very high energy will spiral out, while low energy electrons will circle back to the starting point:

Energy low

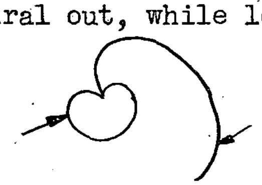

Energy high

Calculations were checked experimentally using thermionic electrons. Fig. 1 illustrates the experimental arrangement and Fig. 2 the trajectories. The dimensions of the detectors must be such as to encompass the entire energy spectrum; at present four crystals in coincidence are used. Figs. 3 and 4 give the intensity distributions--the number of mesons as functions of distance from the axis and from the median plane. The particles are counted in seven separate gates and then totaled.

The mesons are produced by a proton beam incident on a target one inch in diameter. Many of the μ^+ particles are absorbed in the target, while others move back to it after leaving (Fig. 5). Most of the electrons

Fig. 5

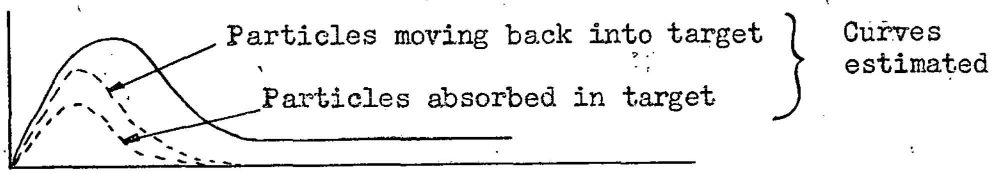

come out of the target. The maximum of the experimental curve concurs with the theory of Tiomno and Wheeler (Fig. 6).

Fig. 6

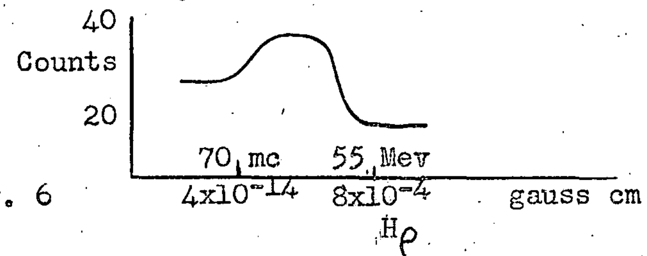

Among the problems yet to be solved are (1) compensating for counts caused by β activity produced inside the target and by the background from $\pi \rightarrow \mu$ which have the same $H\rho$ factor, and (2) scattering of the electrons by the crystals. Crystals of varying thickness have been used with a difference of only 10 percent found in the number of counts, but more work will be done regarding this source of error.

<u>Experiments on Proton-Proton Scattering from 120 to 345 Mev - O. Chamberlain.</u>

Mr. Chamberlain reviewed the work recently completed by Segré, Wiegand and himself on the differential cross section of proton-proton scattering. The results are presented in full in UCRL-1109.

The full strength of the external beam of the 184-inch cyclotron was used as the proton source in the first part of the experiments. The beam current was calibrated with an argon-filled ionization chamber and a Faraday cup as a primary standard. The beam was monoenergetic to one percent. The proton hit a polyethylene or liquid hydrogen target and scattered with an angle of approximately 90° between them. They were counted either singly or in coincidence using stilbene crystal counters; the arrangements are shown in Figs. 7, 8, and 9. The number of counts is given by

$$\text{Counts} = nN\Omega\sigma(\Phi),$$

where n is the number of protons, N the number of hydrogen atoms per cm^2 in the target, Ω the solid angle subtended by the counter and $\sigma(\Phi)$ the differential cross section (Φ is the angle between the direction of the primary beam and a line from the target to the counter). Results are shown in Figs. 10, 11, 12, 13 and 14. Lower energy protons are obtained by passing the beam through lithium absorbers and then collimating it (see Figs. 15 and 16). Larger counting crystals are necessary since the beam is more diffuse.

Many investigators attempt to interpret scattering experiments with velocity independent forces, with reasonable success in fitting the calculated curves with the experimental ones, but work has also been done in which this restriction has been ignored. Evidence in any case is not yet conclusive regarding the charge relationship of nuclear forces.

Information Division
3/8/51 nw

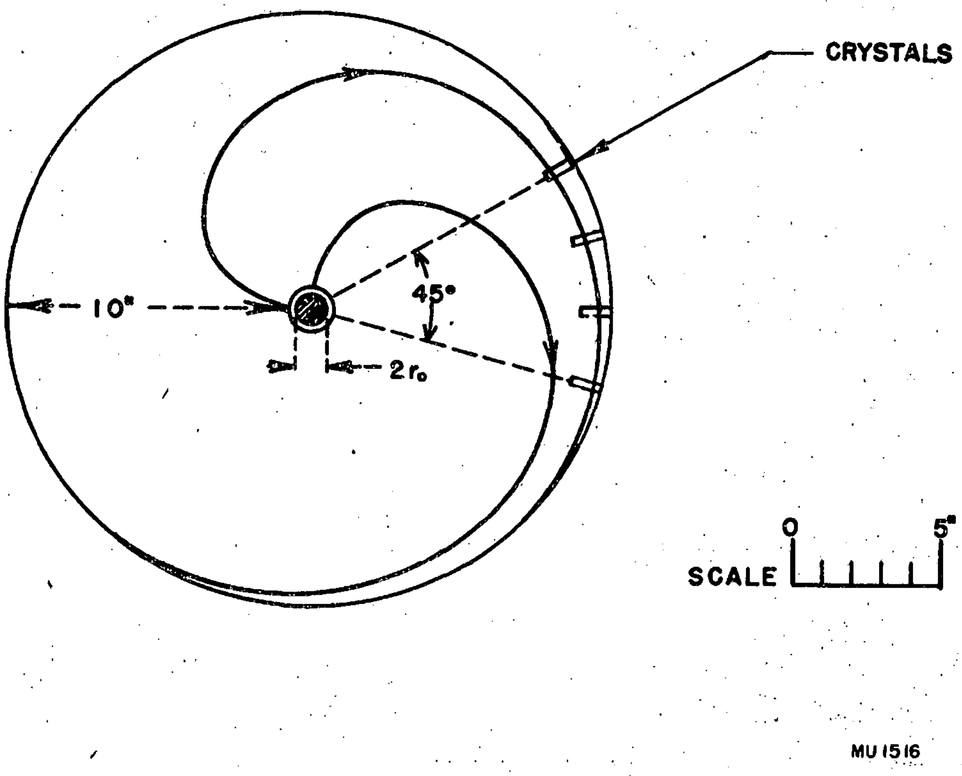

Fig. 1

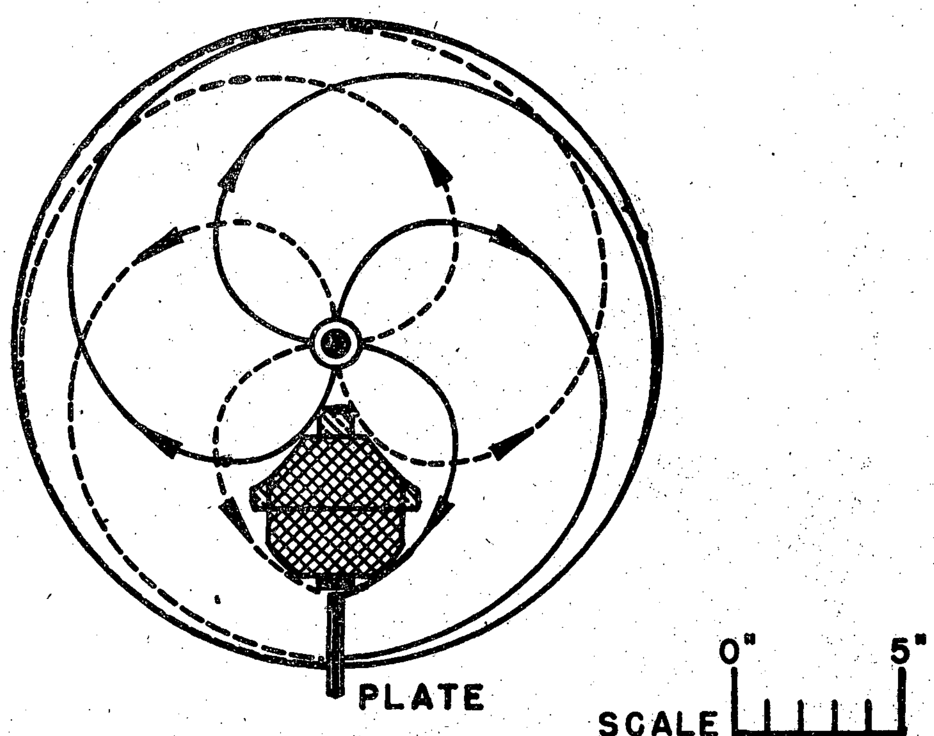

SCHEMATIC DIAGRAM OF TRAJECTORIES

MU 1517

Fig. 2

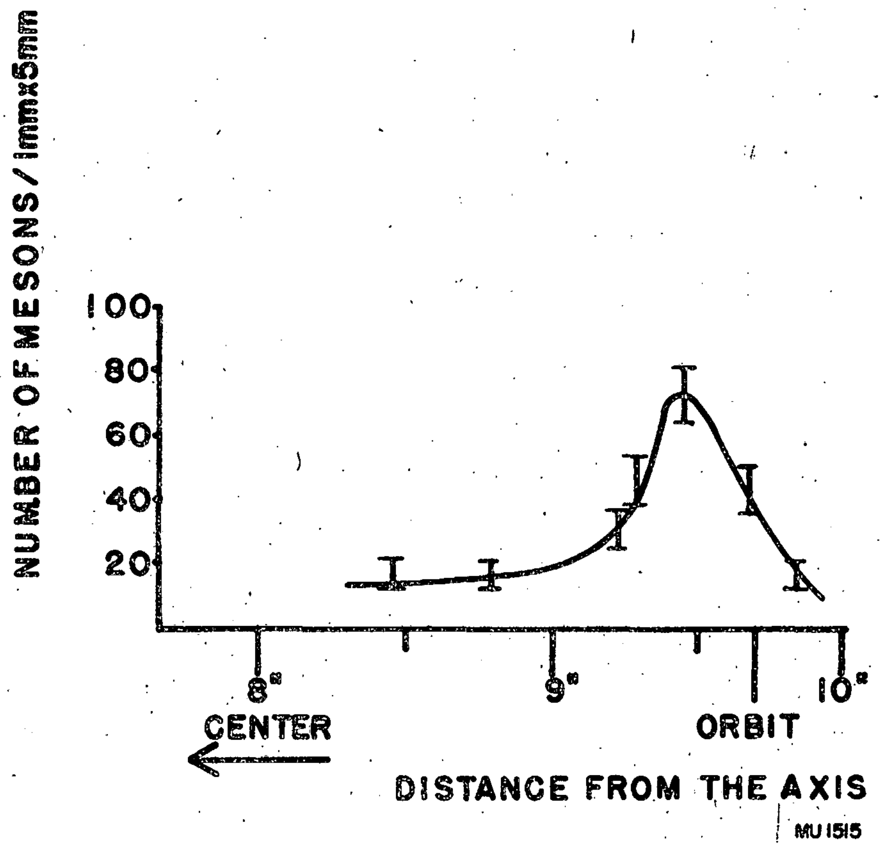
NUMBER OF MESONS / 1mm x 5mm
100
80
60
40
20
8"
9"
10"
CENTER
ORBIT
DISTANCE FROM THE AXIS
MU 1515

Fig. 3

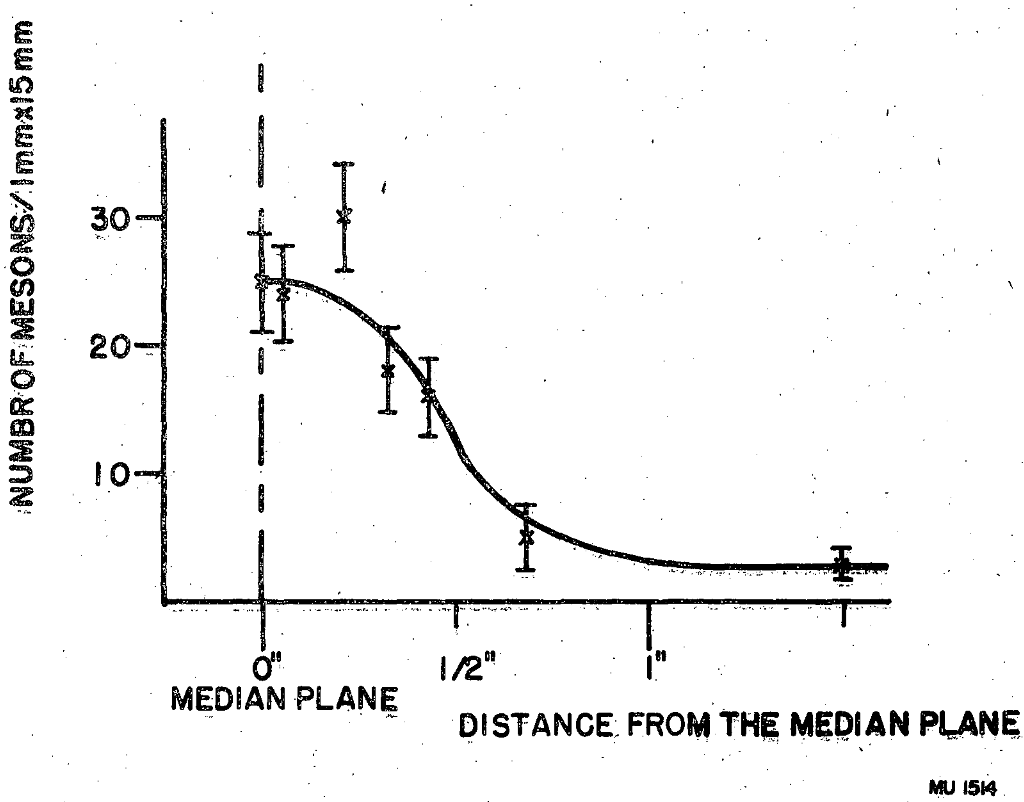
NUMBR OF MESONS/1mmx15mm
30
20
10
0"
MEDIAN PLANE
1/2"
1"
DISTANCE FROM THE MEDIAN PLANE
MU 1514

Fig. 4

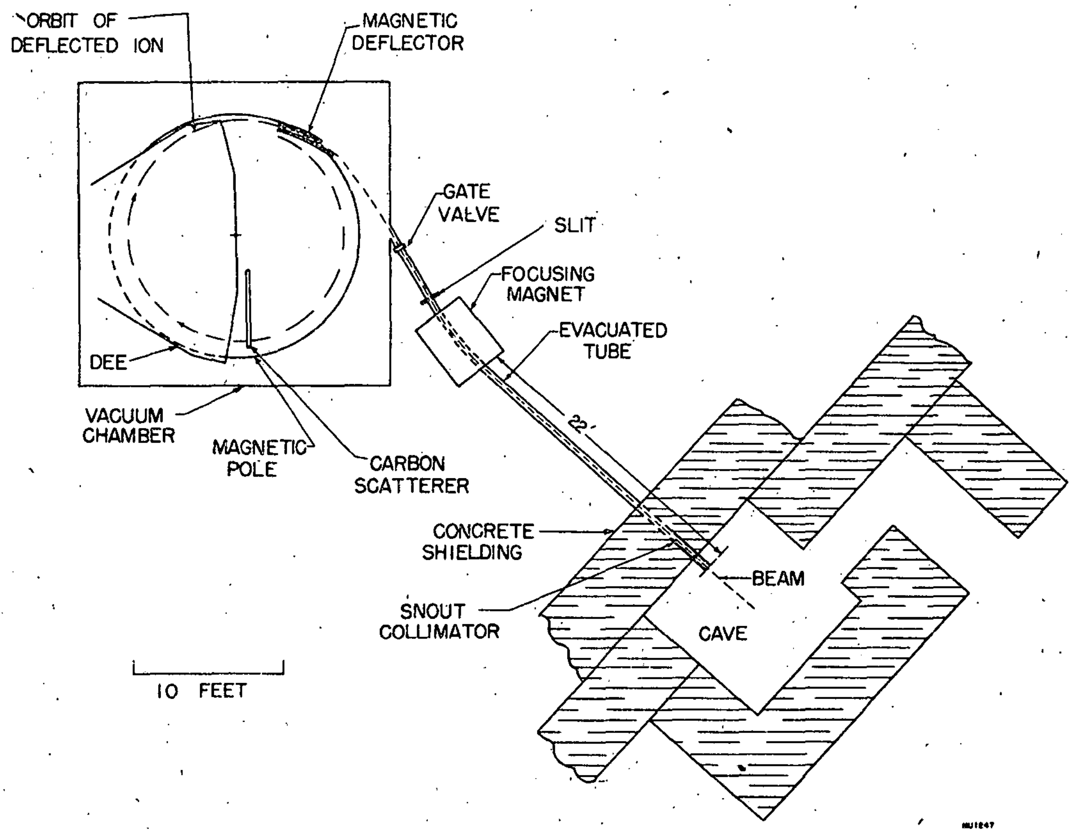
ORBIT OF
DEFLECTED ION
MAGNETIC
DEFLECTOR
GATE
VALVE
SLIT
FOCUSING
MAGNET
EVACUATED
TUBE
22'
DEE
VACUUM
CHAMBER
MAGNETIC
POLE
CARBON
SCATTERER
CONCRETE
SHIELDING
BEAM
SNOUT
COLLIMATOR
CAVE
10 FEET

Fig. 7

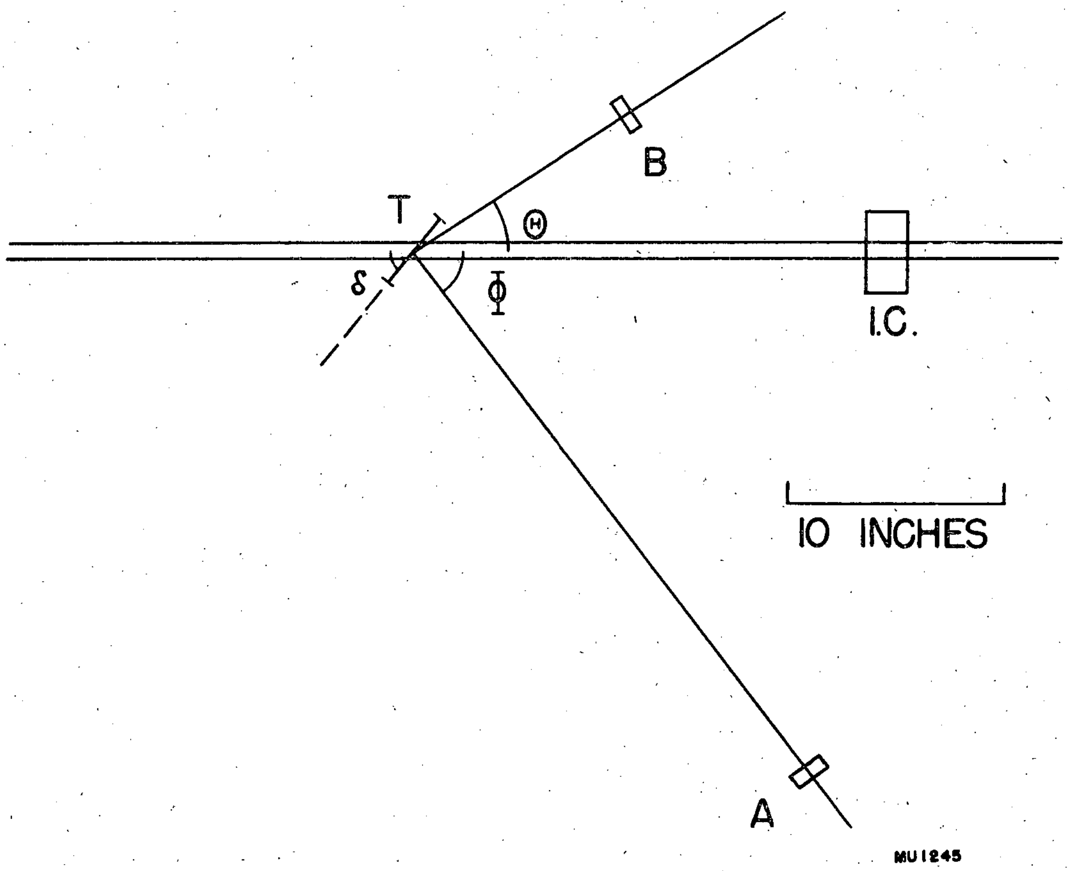

Fig. 8

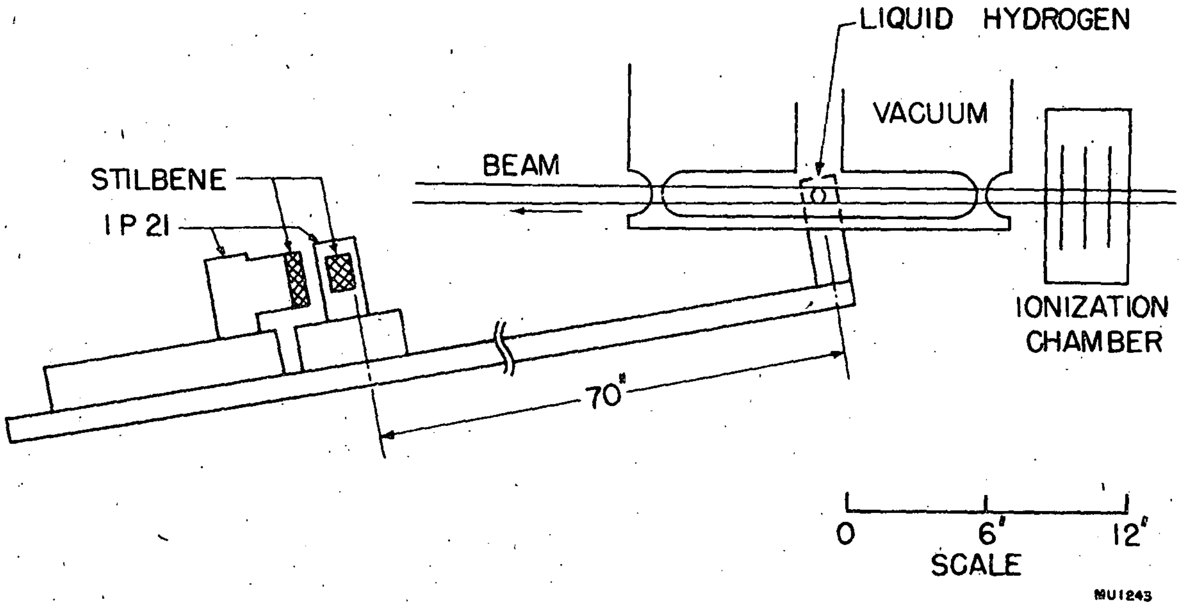
LIQUID HYDROGEN
VACUUM
BEAM
STILBENE
1P21
IONIZATION
CHAMBER
70"
0
6"
12"
SCALE
MU1243

Fig. 9

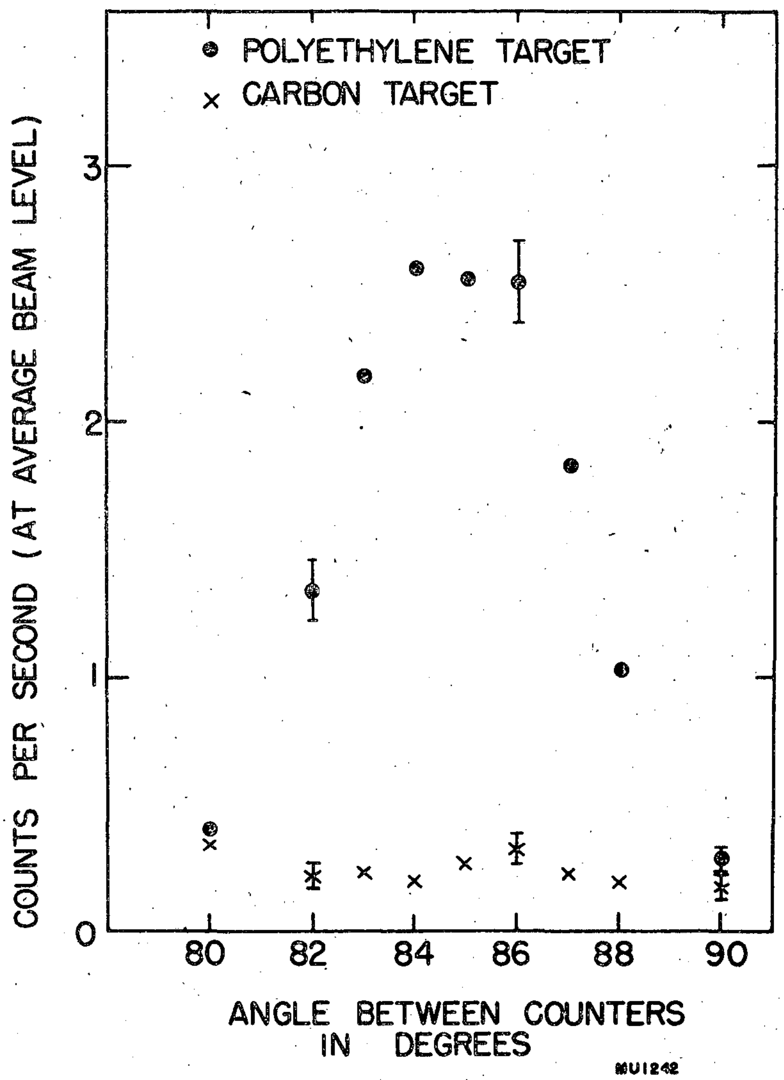

POLYETHYLENE TARGET
CARBON TARGET
COUNTS PER SECOND (AT AVERAGE BEAM LEVEL)
0
1
2
3
80
82
84
86
88
90
ANGLE BETWEEN COUNTERS IN DEGREES
MU1242

Fig. 10

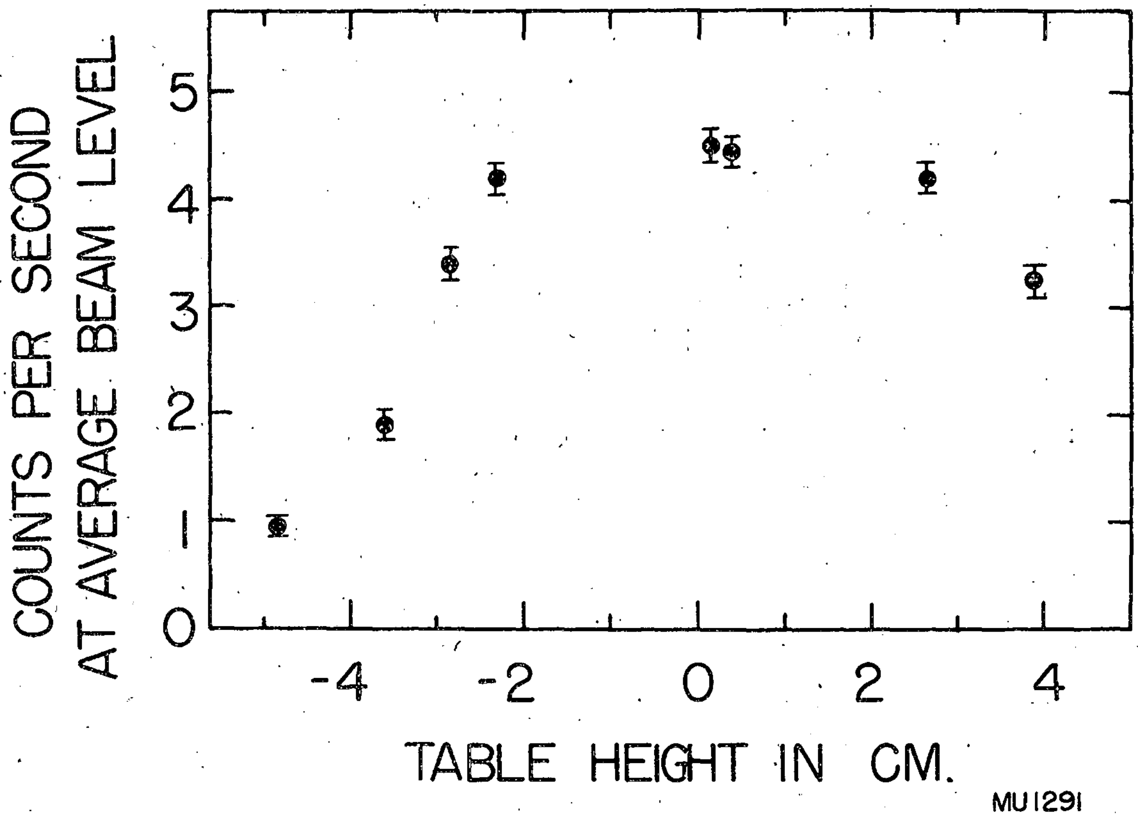
COUNTS PER SECOND
AT AVERAGE BEAM LEVEL
0
1
2
3
4
5
-4
-2
0
2
4
TABLE HEIGHT IN CM.
MU 1291

Fig. 11

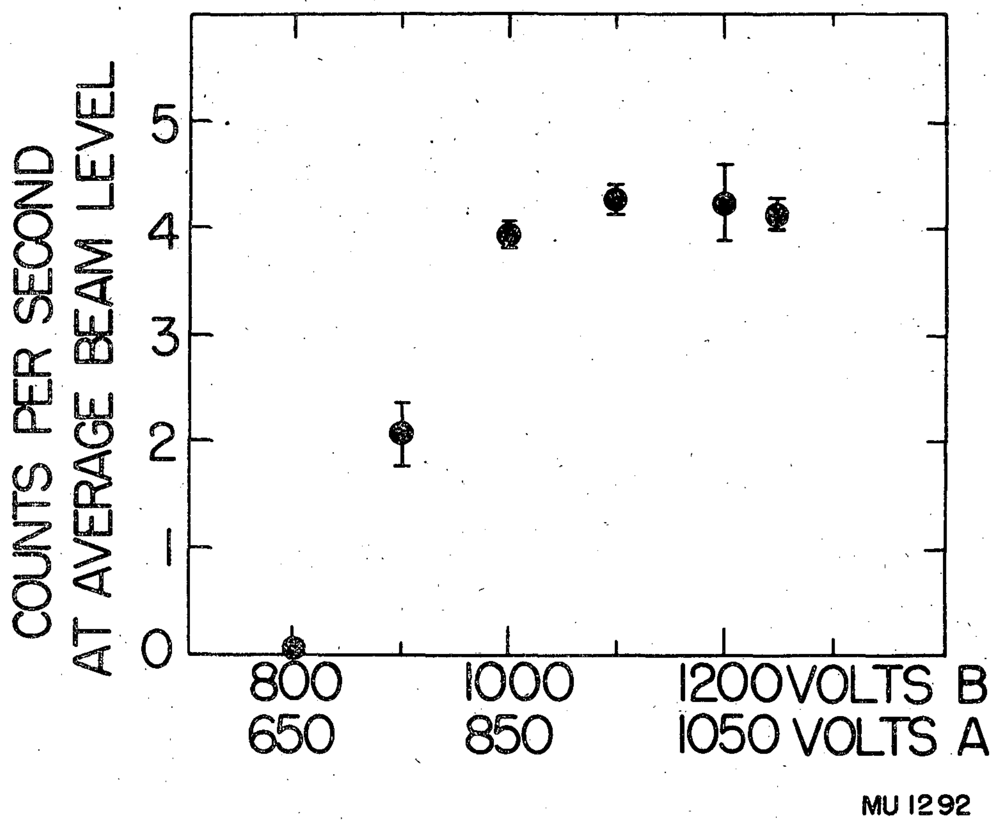
COUNTS PER SECOND
AT AVERAGE BEAM LEVEL
0
1
2
3
4
5
800
650
1000
850
1200 VOLTS B
1050 VOLTS A
MU 1292

Fig. 12

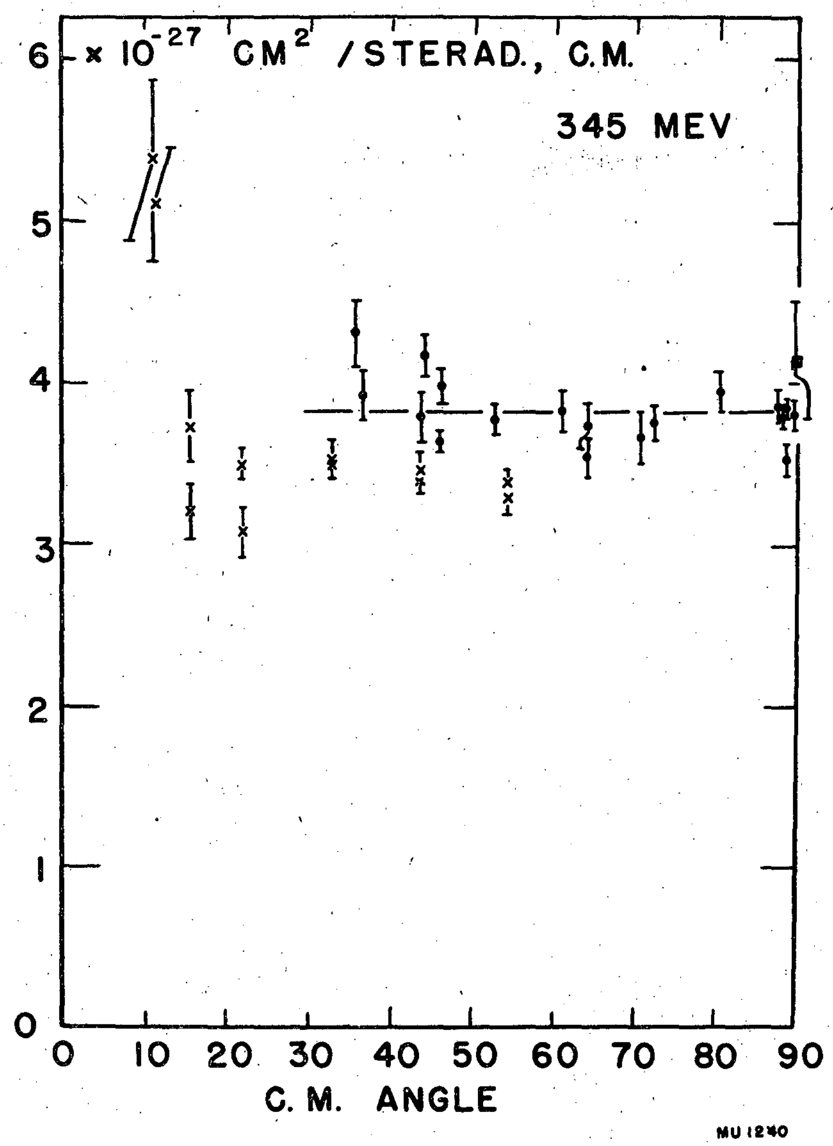
× 10⁻²⁷ CM² /STERAD., C.M.
345 MEV
0
1
2
3
4
5
6
0
10
20
30
40
50
60
70
80
90
C. M. ANGLE
MU 1240

Fig. 13

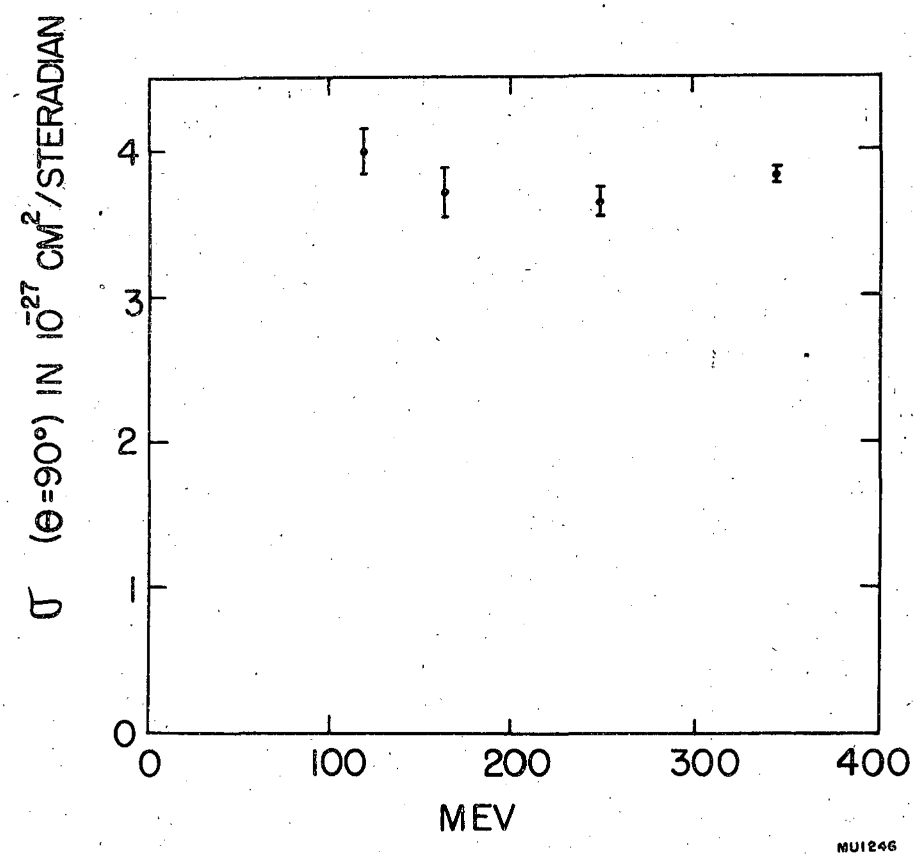

Fig. 14

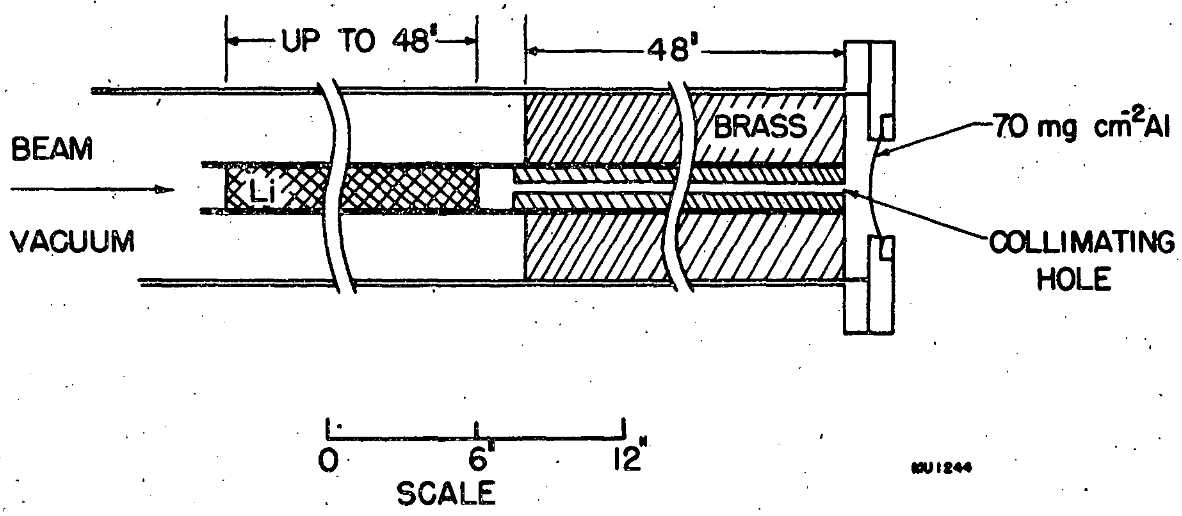
UP TO 48"
48"
BRASS
BEAM
Li
VACUUM
70 mg cm^{-2} Al
COLLIMATING
HOLE
0
6"
12"
SCALE
MU1244

Fig. 15

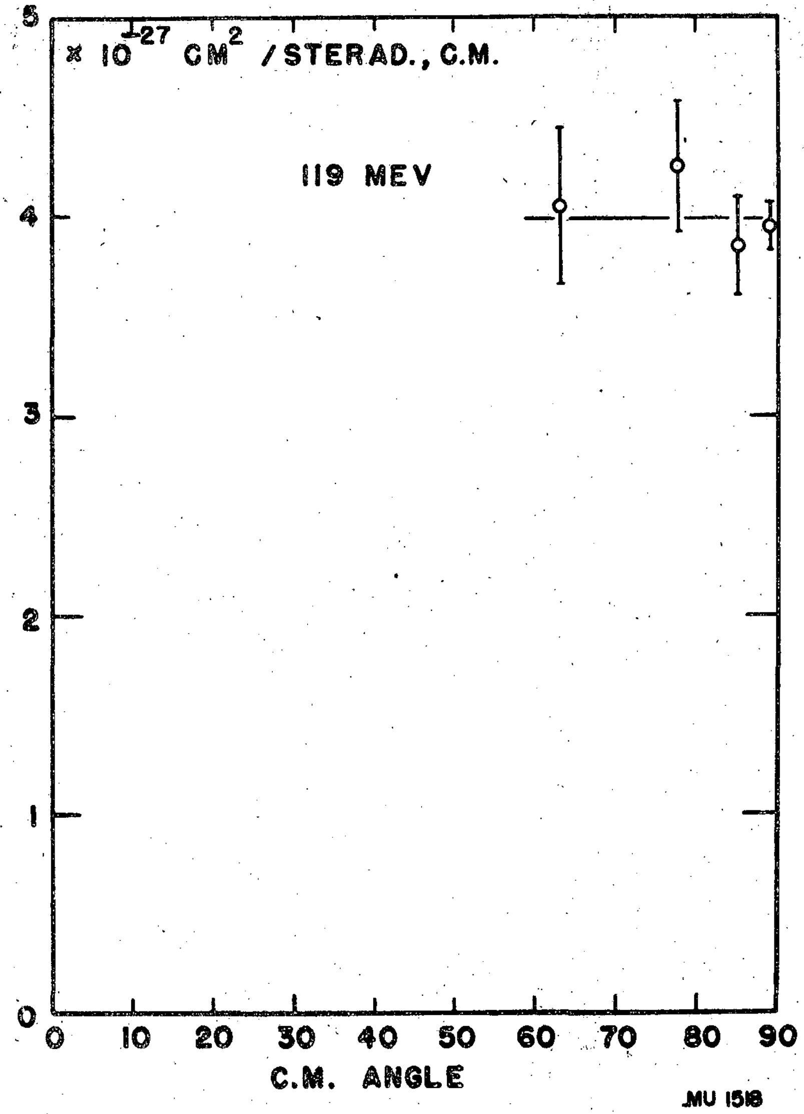

× 10⁻²⁷ CM² / STERAD., C.M.
119 MEV
0
1
2
3
4
5
0
10
20
30
40
50
60
70
80
90
C.M. ANGLE
MU 1518

Fig. 16